Skin Spatial Calibration Using Force/Torque Measurements

Andrea Del Prete, Simone Denei, Lorenzo Natale, Fulvio Mastrogiovanni,
Francesco Nori, Giorgio Cannata, Giorgio Metta

***Abstract*— This paper deals with the problem of estimating the position of tactile elements (i.e. *taxels*) that are mounted on a robot body part. This problem arises with the adoption of tactile systems with a large number of sensors, and it is particularly critical in those cases in which the system is made of flexible material that is deployed on a curved surface. In this scenario the location of each taxel is partially unknown and difficult to determine manually. Placing the device is in fact an inaccurate procedure that is affected by displacements in both position and orientation. Our approach is based on the idea that it is possible to automatically infer the position of the taxels by measuring the interaction forces exchanged between the sensorized part and the environment. The location of the contact is estimated through force/torque (F/T) measures gathered by a sensor mounted on the kinematic chain of the robot. Our method requires few hypotheses and can be effectively implemented on a real platform, as demonstrated by the experiments with the iCub humanoid robot.**

I. Introduction

Nowadays, robots are expected to exhibit advanced features and complex interaction capabilities. For these reasons, recent research work has been focused on the design of robot structures that either take inspiration from the human functional structure [1],[2] or are specifically designed for particular tasks [3]. Furthermore, the design of deeply embedded and functional sensor systems that extend the perception of the surrounding environment has been enforced. In this field, particular attention has been devoted to *tactile sensing*: the key feature for enabling safe human-robot interaction and autonomous tasks in unstructured environments [4],[5].

The development of large-scale tactile sensors requires to deal with several issues that are well beyond the realization of single prototypes. Scalability, conformability [6], wiring [7] and networking [8] are just some of the issues that must be taken into account in the definition of a large scale tactile system able to cover huge parts of a robot body. One possible attempt to solve these issues has been presented in [6] where a network of tactile elements can be applied to arbitrarily curved surfaces. In spite of the low spatial resolution and high power consumption, the solution proposed in [6] allows a simple mechanical integration of transducers on the robot body. In [7], another example of a modular skin has been presented, in which the triangular shape of the sensing modules and the adoption of flexible PCB ensure good conformal properties. Moreover, the modular design allows the skin to be adapted to robot platforms with varying shape and morphology [9].

In spite of the issues discussed above, today we can count on a number of prototypes providing robots with *large-scale*, *skin-like* tactile systems [7]. These devices are characterized by a large number of sensors, which are essential for measuring contacts at high resolution. Dealing with such a large number of tactile units that can be freely placed on a robot has revealed a new class of problems, like folding the skin on the surface to best cover the robot, or the *spatial calibration of the tactile elements*. The latter has been defined in [10] as *the process of finding the location of each tactile element with respect to a known reference frame, after the skin sensor has been actually fixed on a robot body part*. Knowing the location of the tactile elements (i.e., *taxels*) is fundamental to develop complex autonomous behaviours, such as quick response to sudden stimuli or compliant human-robot interaction. Unfortunately the precise location of the taxels is unavailable because the deployment of the tactile device is an imprecise procedure that is affected by unpredictable displacements in both position and orientation. Yet, due to the large number of sensing units, the manual measure of the position of each taxel is tedious and error prone. It is fundamental to realize an automatic or semi-automatic procedure for calibrating the skin once it is placed on the robot.

The design of robots able to learn their own sensory space is not a new problem. In [11], the authors introduce the paradigm of a learning agent able to infer the structure of its sensorimotor system through the interaction with the surrounding environment. This work defines a set of primitives that can be used by a robotic platform to build cognitive maps of the sensor system. A different approach is followed in [12] and [13] where a topological map (rather than a geometric map of taxel locations) is reconstructed. In [12], a method is presented for building an artificial somatosensory map that reflects the spatio-temporal correlations between incoming signals from 250 tactile sensors distributed on the skin of a simulated baby. The result is a map describing the structure of the robot body rather than a set of positions in the robot space. The work presented in [13] is somewhat similar to [12], but it introduces a different approach based on the extraction of features from correlated sensors and it has been tested with real tactile elements on the robotic platform

Giorgio Cannata, Simone Denei and Fulvio Mastrogiovanni are with the Department of Communication, Computer and System Sciences, University of Genova, Via Opera Pia 13, 16145, Genova, Italy. {name.surname}@unige.it.

Andrea Del Prete, Lorenzo Natale, Francesco Nori and Giorgio Metta are with the Robotics, Brain and Cognitive Sciences Department, Italian Institute of Technology, Via Morego 30, 16163, Genova, Italy. {name.surname}@iit.it.

The research leading to these results has received funding from the European Communitys Seventh Framework Programme (FP7/2007-2013) under grant agreement n. 231500/ROBOSKIN.

Robovie-IIF. The correlation between sensors is also used in [14] where an embedding of sensors is performed, that is, in this paper, a mapping between the sensors space and a Euclidean space. The author shows that, after defining a sensor correlation distance, it is possible to build a representation of sensors that preserve the computed distances, with the technique of Maximum Variance Unfolding. Although the results show a reconstruction of the geometry of the sensors placed on a 3D model with different curvatures and holes, the constructed map does not correspond to real sensor positions, but it is a scaled version resembling the original shape. An example of an automatic procedure for calibrating a robot skin can be found in [10] where, under some somewhat tight assumptions, the authors show a calibration method that is based on the compliant motion between a robot and an external object with known shape. Although the results reported in the paper show the feasibility of the approach in simulation, this work makes some simplifying hypothesis and assumes a certain prior knowledge about the environment and, overall, it seems difficult to replicate on a real robotic platform.

With the sole exception of [10] all the available calibration techniques produce maps that are topological. Unfortunately for such tactile maps to be useful for control (at least considered the control systems commonly implemented in robotics) it is necessary to provide robots with metric information, rather than only topological.

The major contribution of this paper is a method for the geometrical calibration of robot skin in 3D space. Our method can be implemented on any robot platform that is equipped with a sensor that is able to measure forces and torques on the part of the body that requires calibration. The experimental section shows that this technique allows the estimation of the positions of the taxels with good precision (average error of about 7 mm). This can be further improved if knowledge of the shape of the robot is available.

The paper is structured as follows: Section II describes the proposed method for estimating the taxel positions; Section III provides details on the test platform used in the experiments. Finally Section IV and Section V report and discuss the results of the paper.

II. Determining Taxel Positions Through Force/Torque Sensor Measurements

The proposed approach is based on the idea that it is possible to determine where the taxels are placed by applying forces on the sensorized part. In fact, under some assumptions, by measuring the resulting forces and torques on the body part it is possible to determine the point of application of the forces (i.e., the contact point). If we apply forces that activate a small set of sensors near the point of application of the force, the measured point of contact provides an estimation of the position of the activated taxels.

The problem of determining the contact location, given force and torque measurements, has been already investigated in the literature [15],[16]. When arbitrary forces and moments are applied to a body and only the measures of a single sensor attached to the body are available, it is hard to derive the contact geometry and, as a consequence, to determine each contact point. Let us consider for instance a sensor measuring forces and torques on a rigid body, on which n wrenches are applied at different locations $\mathbf{c}_u \in \mathbb{R}^3$, $u = 1, \ldots, n$ (expressed w.r.t. the sensor reference frame). The equations relating forces $\mathbf{f}_{c_u}$ and moments $\mathbf{m}_{c_u}$ applied to the body, with the force and moment measured by the F/T sensor, respectively $\mathbf{f}_s$ and $\mathbf{m}_s$, are:

$$\mathbf{f}_s = \sum_{u=1}^{n} \mathbf{f}_{c_u},$$

$$\mathbf{m}_s = \sum_{u=1}^{n} (\mathbf{m}_{c_u} + \mathbf{c}_u \times \mathbf{f}_{c_u}).$$

In the hypothesis that only a single contact point $\mathbf{c}$ exists, no torque can be applied to the body (i.e. $\mathbf{m}_c = 0$). In this case, the number of unknowns of the problem decreases, and some information about the contact point can be retrieved [15]:

$$\mathbf{f}_s = \mathbf{f}_c, \tag{1}$$

$$\mathbf{m}_s = \mathbf{c} \times \mathbf{f}_c. \tag{2}$$

The assumption $\mathbf{m_c} = 0$ can be easily verified. In fact, from (1) and (2) it follows that:

$$\mathbf{f}_s \mathbf{m}_s = 0. \tag{3}$$

Now, substituting (1) in (2) leads to:

$$\mathbf{m}_s = \mathbf{c} \times \mathbf{f}_s, \tag{4}$$

which is a three equation system, where the only unknowns are the three coordinates of the contact point $\mathbf{c}$. The system can not be completely solved, because the three equations are not independent. However, we can determine the force axis r:

$$\mathbf{c} \in \left\{ \frac{\mathbf{f}_s \times \mathbf{m}_s}{||\mathbf{f}_s||^2} + \lambda \mathbf{f}_s \right\} = r, \qquad \forall \lambda \in \mathbb{R},$$

where λ is a free variable and $||.||$ is the Euclidean norm.

Suppose that we are applying a sequence of pure forces to the sensorized robot body part; we can define the set of all the h measured wrenches $\mathbf{w}_{s_i} \in \mathbb{R}^6$, $i = 1, \ldots, h$ as:

$$W_s = \{\mathbf{w}_{s_1}, \mathbf{w}_{s_2}, \ldots, \mathbf{w}_{s_h}\},$$

$$\mathbf{w}_{s_i} = \begin{bmatrix} \mathbf{f}_{s_i} \\ \mathbf{m}_{s_i} \end{bmatrix}.$$

For estimating the position $\mathbf{p}_j$ of the j-th taxel we can use only the subset of W_s defined as:

$$\tilde{W}_j = \{\mathbf{w}_{s_i} \in W_s : \ {}^i t_j > \delta\}, \qquad j \in \{1, \ldots, d\}$$

where d is the number of taxels, ${}^i t_j$ is the output of the j-th taxel with respect to the i-th force applied, and δ is an experimentally determined constant parameter (i.e., a threshold) used for discriminating a contact response from the noise of the sensor.

At this point we have two options for computing the taxel locations starting from force axes. The first method,

described in Section II-A, does not require the knowledge of the robot surface. The second method, described in Section II-B, assumes that we have a mathematical description of the robot body part, or, in other words, that we only need to determine the position of each taxel on the surface.

A. *Contact point estimation without knowing the robot shape*

Let us consider an ideal scenario where a sequence of single point contacts, occurring at different locations $\mathbf{c}_i$, activates one taxel at a time. In this case it is possible to identify the location of a taxel, if more than a single measure – originating from the same taxel – is available. In fact as soon as two force axes are determined, their intersection locates the taxel. However, the F/T measures are subject to noise and this may cause errors in the position and orientation of the force axis. Moreover, the hypothesis of single contact point does not hold in practice, and an undesired moment $\mathbf{m_c} \neq 0$ may introduce further errors in axis estimation. Furthermore, given the resolution of the skin, around 3 taxels per cm^2 in our tests (see Figure 3), different contact locations can activate the same taxel and provide different contributions to the estimation of the taxel position.

One way to tackle these issues, is to collect a large number of measures (i.e., wrenches) and determine the point that best approximates the intersection of the related force axes, to finally get an estimate of the real location of the taxel. We solve this problem using a least squares procedure [17]. Formally, starting from (4) and considering the n_j wrenches $\tilde{\mathbf{w}}_{s_r} \in \tilde{W}_j$, $r = 1, \ldots, n_j$ corresponding to the same taxel j, we can define the following system of equations:

$$\underbrace{\begin{bmatrix} S(\frac{\tilde{\mathbf{f}}_{s_1}}{||\tilde{\mathbf{f}}_{s_1}||}) \\ S(\frac{\tilde{\mathbf{f}}_{s_2}}{||\tilde{\mathbf{f}}_{s_2}||}) \\ \vdots \\ S(\frac{\tilde{\mathbf{f}}_{s_{n_j}}}{||\tilde{\mathbf{f}}_{s_{n_j}}||}) \end{bmatrix}}_{[F\times]_j \in R^{3n_j \times 3}} \mathbf{p}_j = - \underbrace{\begin{bmatrix} \frac{\tilde{\mathbf{m}}_{s_1}}{||\tilde{\mathbf{f}}_{s_1}||} \\ \frac{\tilde{\mathbf{m}}_{s_2}}{||\tilde{\mathbf{f}}_{s_2}||} \\ \vdots \\ \frac{\tilde{\mathbf{m}}_{s_{n_j}}}{||\tilde{\mathbf{f}}_{s_{n_j}}||} \end{bmatrix}}_{M_j \in R^{3n_j \times 1}}, \tag{5}$$

where $S(\mathbf{v}) \in R^{3\times3}$ is the operator performing the cross product $\mathbf{v}\times$. We divided both sides of (4) by the module of the force, so as to avoid weighting the contribution of each axis proportionally to the module of the relative force. In the end the sum of the squares of the residual is:

$$\begin{aligned} R_j &= \sum_{r=1}^{n_j} \left(\frac{||\tilde{\mathbf{f}}_{s_r} \times \mathbf{p}_j + \tilde{\mathbf{m}}_{s_r}||}{||\tilde{\mathbf{f}}_{s_r}||} \right)^2 \\ &= \sum_{r=1}^{n_j} \left(\frac{||\tilde{\mathbf{f}}_{s_r} \times ({}^r\hat{\mathbf{p}}_j + {}^r\mathbf{e}_j) + \tilde{\mathbf{m}}_{s_r}||}{||\tilde{\mathbf{f}}_{s_r}||} \right)^2 \\ &= \sum_{r=1}^{n_j} \left(\frac{||-\tilde{\mathbf{m}}_{s_r} + \tilde{\mathbf{f}}_{s_r} \times {}^r\mathbf{e}_j + \tilde{\mathbf{m}}_{s_r}||}{||\tilde{\mathbf{f}}_{s_r}||} \right)^2 \\ &= \sum_{r=1}^{n_j} \left(\frac{||\tilde{\mathbf{f}}_{s_r} \times {}^r\mathbf{e}_j||}{||\tilde{\mathbf{f}}_{s_r}||} \right)^2 = \sum_{r=1}^{n_j} ||{}^r\mathbf{e}_j||^2, \end{aligned}$$

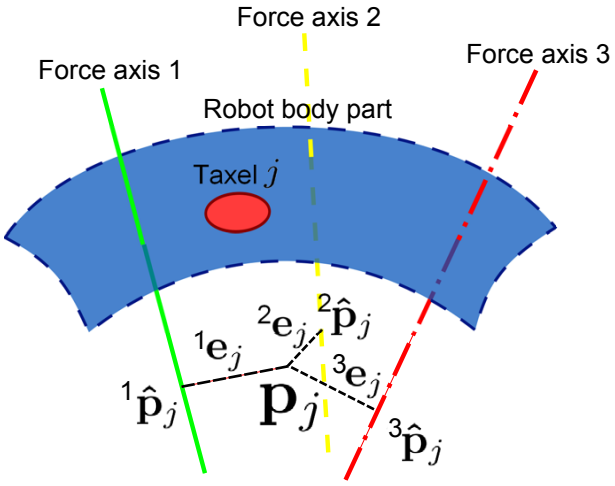

Fig. 1. The j-th taxel estimated position $\mathbf{p}_j$ obtained with the Least Square Technique. In this case, the estimate is not constrained to be on the surface.

where we decomposed $\mathbf{p}_j$ into the sum of its projection on the r-th force axis ${}^r\hat{\mathbf{p}}_j$, and its distance from the r-th force axis ${}^r\mathbf{e}_j$ (see Fig. 1). The least squares estimate of the j-th taxel position $\mathbf{p}_j$ can be obtained as:

$$\mathbf{p}_j = -\left([F\times]_j^T [F\times]_j \right)^{-1} [F\times]_j^T M_j,$$

where we assume that $[F\times]_j$ has full rank (i.e. $rank([F\times]_j) = 3$). This assumption is reasonable, given the large number of rows of the matrix, and besides it is easy to verify.

Consider now a more realistic scenario, in which each contact turns out to activate more than a single taxel at the same time. Since the taxels are quite close to each other (about 5.5 mm from the two centres, see Figure 3) this happens most of the time. Obviously enough, a number of taxels are closer than others to the actual contact point, hence they should not be treated in the same way. This aspect can be modelled by introducing a weight for each active taxel, that is proportional to its distance from the contact location. Of course the real distance between the taxels and the contact point is not known, but we do know that the closer a taxel is to the contact point, the greater its response. Formally, for each measure in $\tilde{W}_j$ we can define the weight associated to the taxel j as:

$${}^rk_j = \frac{{}^rt_j}{\max\limits_{y=1\ldots d}({}^rt_y)},$$

where ${}^rt_y$ is the output of the y-th taxel with respect to the r-th wrench in $\tilde{W}_j$, and $\max_y({}^rt_y)$ is the maximum of all the activated taxel outputs with respect to the r-th wrench. We construct a diagonal weighting matrix $K_j \in R^{3n_j \times 3n_j}$ whose diagonal coefficients are ${}^rk_j$ (each appearing three times), and compute the solution of a Weighted Least Squares problem [17] as:

$$\mathbf{p}_j = -\left([F\times]_j^T K_j^2 [F\times]_j \right)^{-1} [F\times]_j^T K_j^2 M_j.$$

The points $\mathbf{p}_j$ so computed are expressed w.r.t. the F/T sensor reference frame $<s>$, depicted in Fig. 2. If $<s>$is not fixed

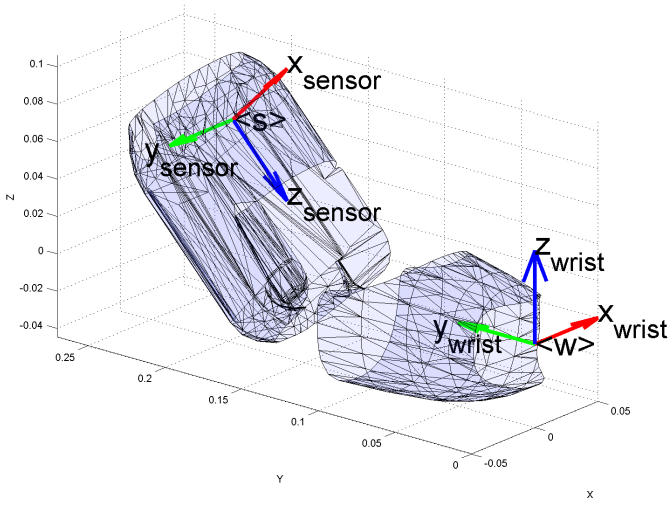

Fig. 2. F/T sensor reference frame $<s>$and wrist reference frame $<w>$. The F/T sensor is located inside the upper part of the iCub arm, hence the two degrees of freedom of the iCub elbow affect the position of $<w>$w.r.t. $<s>$. In this figure the two joint angles of the elbow (j_3, j_4) are set to $45°$ and $0°$. The remaining joints j_0, j_1, j_2 are located before the F/T sensor in the arm kinematic chain, hence they affect the position of the whole arm.

w.r.t. the taxel positions, but the relative roto-translation is known, we can represent the points w.r.t. another reference frame. In our case we chose the wrist reference frame $<w>$, which is fixed w.r.t. the forearm of the robot. By doing so, wrenches collected with different arm configurations can be used at the same time in (5). Denoting with ${}^a\mathbf{v}$ a vector $\mathbf{v} \in \mathbb{R}^3$ expressed in the reference frame $<a>$, we represent the points on the wrist reference frame $<w>$:

$$ {}^s\mathbf{p} = {}^s\mathbf{o}_w + {}^s_wR\,{}^w\mathbf{p}, \tag{6} $$

where ${}^s\mathbf{o}_w$ is the origin of $<w>$ expressed w.r.t. $<s>$, and ${}^s_wR \in R^{3\times3}$ is the rotation matrix from $<s>$ to $<w>$. Substituting (6) in (4) we get:

$$ {}^s\mathbf{f} \times {}^s_wR\,{}^w\mathbf{p} = -{}^s\mathbf{m} - {}^s\mathbf{f} \times {}^s\mathbf{o}_w. $$

Finally the least squares problem in (5) can be easily reformulated starting from this new equation.

B. Contact point estimation knowing the robot shape

If we know the shape and the position of the surface where the skin is placed, we can exploit this information to constrain the taxel position estimates on that surface. A least squares problem in which the unknowns are required to satisfy a system of equality and inequality constraints may be solved using a Constrained Least Squares procedure [17]. In our case, we know the mathematical description of the triangles that form a mesh that approximates the cover of the robot arm. We can force the point to belong to a triangle by imposing four linear constraints: one equation for the plane and three inequalities for the three edges of the triangle. The problem is solved separately for every triangle and, in the end, the solution with the minimum sum of the squares of the residuals is chosen.

III. Test Platform

The proposed method has been tested on the humanoid robot iCub. The iCub is an open software/hardware robotic platform, aimed at the study of embodied cognition [1]. Its high number of degrees of freedom (53 in total, 30 in the upper body of which 9 just in each hand) and its small height of 104 cm, distinguish this robot from the other humanoid platforms worldwide. A large variety of sensors are mounted on the robot: digital cameras, gyroscopes and accelerometers, microphones, force/torque sensors and a distributed sensorized skin.

A. The force/torque sensor

The iCub is equipped with four custom made F/T sensors [18], each one located in each limb. The location of the sensors differs from the usual distal configuration at the end effector. Indeed they are located in between the shoulder and the elbow in the arm, and in between the knee and the hip in the legs. The solution allows the measurement of both internal dynamics and external forces exerted on the whole limb, in contrast with the distal configuration, whose measurements would be limited to the end-effector.

B. The robot skin

A compliant skin incorporating a distributed pressure sensor, based on capacitive technology, is currently mounted on the iCub arms, palms and fingertips [9] (see Fig. 3). The skin is organized in triangular modules, except for the

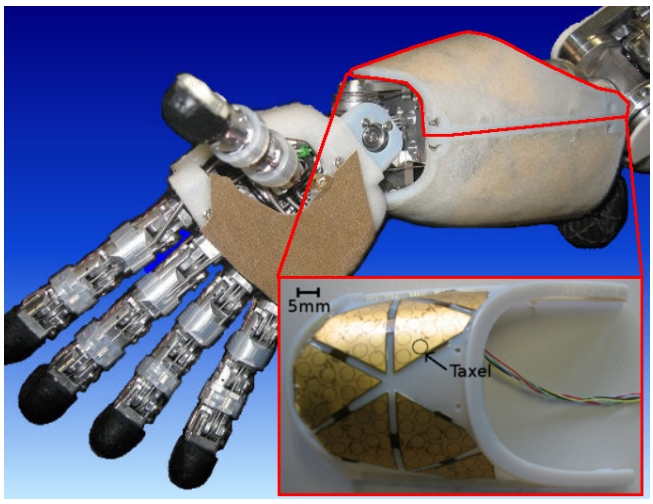

Fig. 3. Right arm of the iCub robot, with skin mounted on the forearm, palm and fingertips. In the red box, the lower forearm cover equipped with Roboskin[7]. This part is not covered with the silicone foam yet.

fingertips, where a particular solution has been designed for complying with the small size and round shape. Each module, composed by 12 taxels (see Figure 3), is able to scan locally 12 measurements of capacitance and send them through a serial bus.

The basis of the sensor is a flexible printed circuit board (PCB). A 2/3 mm thick layer of silicone foam is placed above the PCB, covering the 12 taxels. The role of this layer is two-fold: (i) it acts as a deformable dielectric for the capacitive

pressure sensor and (ii) it makes the skin compliant. In the hands a second conductive layer is placed on top of the silicon foam, in order to make the sensors sensitive to every material, regardless of its electrical properties. At the time the experiments on this paper were conducted the skin on the arm was under development, and the conductive layers on the arms of the robot were not mounted. For this reason the contact on the skin was elicited using a metal tool.

In every skin triangle the 12 taxels can be read either independently at 50 Hz, or as an average of them at about 500 Hz.

IV. Experimental Results

The two proposed approaches have been tested on the skin of the right forearm of the iCub. The *single point contact* has been approximated by poking the robot skin using a metal tool, with a flat square tip. This tool has been preferred to the human finger because of its small tip (about 4x4 mm), which on average activates just three taxels at a time, as opposed to seven.

We collected several datasets, each corresponding to a different configuration of the arm. During each data collection the robot was controlled to keep a fixed position. The external wrench has been computed as the difference between the wrench measured by the F/T sensor and the constant wrench due to the weight of the arm. Several arm positions have been considered (see Table I), so as to span a significant variety of arm configurations. It is worth to note that only

TABLE I

Joint angles of the shoulder (j_0, j_1, j_2) and the elbow (j_3, j_4) set during the tests

N	Duration (min)	j_0 -95:10	j_1 0:160	j_2 -37:80	j_3 15:106	j_4 -90:90
1	13	-10	20	20	94	0
2	5	-30	30	0	15	-90
3	4	-30	30	0	35	-40
4	7	-10	20	20	94	0
5	7	-30	30	0	94	0
6	7	-10	20	20	45	0
7	7	-10	20	20	94	-90

the two elbow joints, j_3 and j_4, affect the position of the forearm with respect to the F/T sensor reference frame.

To assess the two methods, a reference model of the taxel positions have been compared with the results, measuring the displacement of every taxel from its expected location.

A. Single dataset

The data collected in each test (see Table I) have been processed individually with both the proposed methods, leading to quite diverse results, reported in Fig. 4. For the first method the mean error ranges from 8.1 mm to 18.5 mm, with the standard deviation going from 4.2 mm to 8.3 mm. For the second method the mean error ranges from 5.2 mm to 19.3 mm, with the standard deviation going from 3.1 mm to 13.1 mm. The significant differences between the

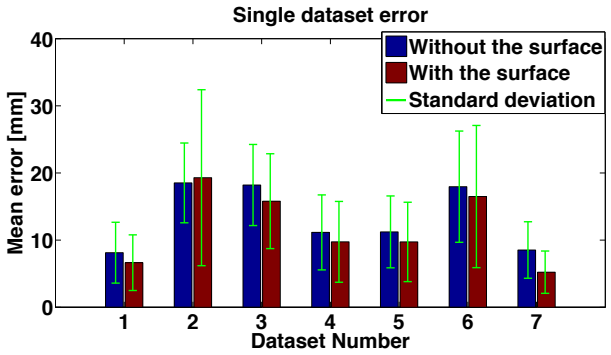

Fig. 4. Mean and standard deviation of the error of the 84 taxel estimations, computed for every dataset. The red bars show the error of the results obtained constraining the points on the skin surface, whereas the blue bars represent the error obtained without using the surface. As expected the results improve when the surface constraint is imposed.

various datasets can be attributed to the F/T measurements, whose precision varies depending on the magnitude of the forces and torques that are measured. These, in turns, depend on the arm configuration. By comparing the two methods it is clear that constraining the points on the skin surface generally improves the results, even if in one case (dataset 2) the opposite occurs.

B. All datasets

If all the estimated taxel positions are represented with respect to the same reference frame, it is possible to compute their average to derive a more accurate estimation. This was computed iteratively. In other words at each step the taxel positions found using a new dataset were averaged with the current position estimations. The results of the average for both the proposed methods are depicted in Fig. 5. In both

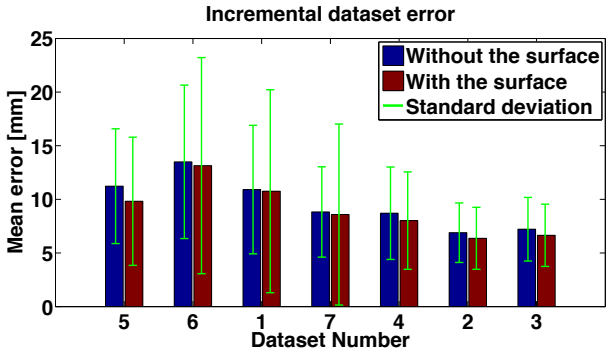

Fig. 5. Mean and standard deviation of the error of the 84 taxel estimations computed after the estimation from each dataset is incrementally averaged. The red and blue bars show the error of the results obtained respectively with or without constraining the points on the skin surface. The estimation improves as more data are computed. The final mean error is 6.6 mm for the "surface case", and 7.2 mm for the "no surface case". The max error is 18.5 mm without the surface and 19.4 mm with the surface.

cases the quality of the result improves as more data are added to the average, leading to a final average error of 7.2 mm for the first method and 6.6 mm for the second method. As expected the precision of the results improves

when the knowledge of the surface is employed to constrain the solution of the minimization.

It is worth noticing that for the first method the final error (mean 7.2 mm, standard deviation 3 mm) is better than the best of the errors obtained from the single datasets, (mean 8.1 mm, standard deviation 4.2 mm). For the second method this did not happen, because the final error (mean 6.6 mm, standard deviation 2.9 mm) is worse than the error obtained with the single dataset 7 (mean 5 mm, standard deviation 3.1 mm). Nonetheless, considering the wide range of errors resulted from the single datasets – up to 19.3 mm – the error obtained merging all the estimations can still be regarded favourably.

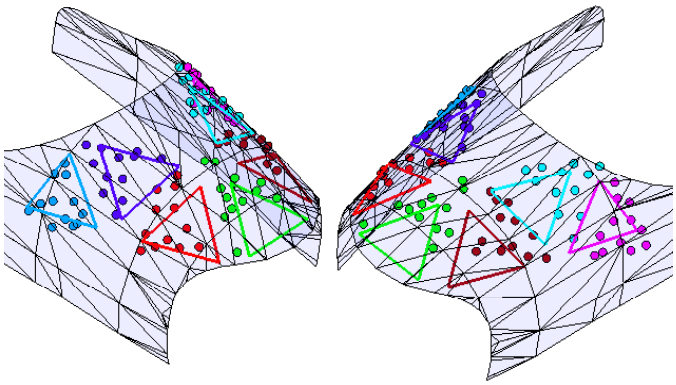

Fig. 6. Final taxel position estimations obtained constraining the points on the skin surface. As reference, the edges of the seven skin triangles are drawn over the forearm surface. The same colours are used to draw the triangles and the corresponding (estimated) taxels. Two views of the same result are depicted, to better show the taxel positions.

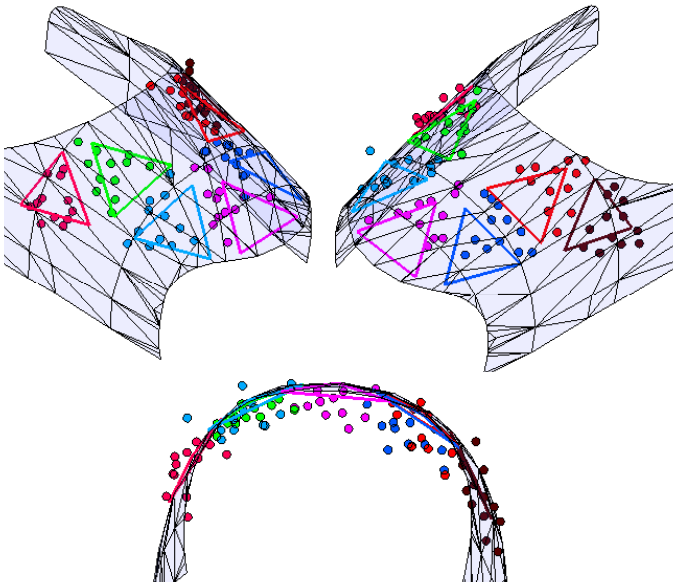

Fig. 7. Final taxel position estimations obtained without constraining the points on the skin surface. As reference, the edges of the seven skin triangles are drawn over the forearm surface. The same colours are used to draw the triangles and the corresponding (estimated) taxels. Three views of the same result are depicted, to better show the taxel positions.

Finally, to better visualize the results, in Fig. 6 and 7 we plot the estimated taxel positions obtained using all the datasets, respectively with and without constraining the points on the arm surface.

C. Error analysis

To complete the assessment of the methods, some words should be spent regarding the sources of error. The quality of the taxel position estimation depends on several aspects, and most of them resides in the robotic platform rather than in the method itself. First of all, errors in the force and torque measurements, respectively ε_m and ε_f, directly affect the estimate, turning equation (4) into:

$$\mathbf{m}_s + \varepsilon_m = \hat{\mathbf{c}} \times (\mathbf{f}_s + \varepsilon_f).$$

Hence the estimated force axis is equal to:

$$\hat{\mathbf{c}} \in \left\{ \frac{(\mathbf{f}_s + \varepsilon_f) \times (\mathbf{m}_s + \varepsilon_m)}{||\mathbf{f}_s + \varepsilon_f||^2} + \lambda(\mathbf{f}_s + \varepsilon_f) \right\} = \hat{r}.$$

Clearly if ε_m and ε_f are too large the estimated force axis will be too distant from the contact point, resulting in a large error in the taxel position estimations.

Uncertainties in the kinematics model of the robot affect the position estimate. As it can be seen in equation (6), to use all the datasets taken in different poses of the robot arm, the taxel positions have to be expressed w.r.t. a common fixed reference frame. An error in the transformation between the F/T sensor reference frame and the common reference leads to a wrong estimate of the taxel position.

The proposed approach makes some hypotheses that do not hold completely in real scenario. Although the robot has been poked with a small tip tool, the contact type is surely not a single point contact, thus introducing further uncertainty in the localization. Moreover, the method estimates the taxel positions by trying to find the point that best approximates the intersection among axes of different forces. If the axes are almost parallel the problem is ill-posed, thus much more sensitive to errors in the input data.

V. Conclusions And Future Work

This paper describes two methods for the estimation of the position of tactile sensing elements on robot body parts. Differently from previous works [12] [13] [14], these methods estimate not only the network topology, but also the location of each sensor with respect to a known reference frame. This is a crucial point if the sensor data has to be integrated with other information (e.g. kinematics, force/torque sensor measures) for controlling the robot.

The first presented approach does not require the knowledge of the robot surface. By averaging the results of the estimation from different arm configurations, this procedure allows to determine the position of each taxel with an average error of 7.2 mm. This can be further reduced to 6.6 mm in case the shape of the robot surface is known, as it can be appreciated qualitatively by looking at the reconstruction in Fig. 6. These results are remarkable, considered that the calibration requires few hypothesis and that it is performed on a real robot using noisy data (the robot kinematics and

the F/T sensor measures). The second approach assumes that a mathematical description of the surface on which the skin is placed is available, so as to constrain the taxel position estimations on it. This assumption is reasonable, since the surface of the robot can be derived once from the CAD model of the robot, and is independent of how the skin is mounted.

As it can be noticed in Fig. 7 the contact areas are not localized precisely, but the neighbouring relationships between taxels are preserved (taxels that are neighbours in the real sensor network are neighbours in the network reconstruction too). The precision achieved is anyway sufficient for understanding where contacts occur on the robot body. This is important information that can be used, for instance, to implement reactive movements, where imprecise knowledge of the contact location is enough for reacting in the proper way. The causes of the errors, as discussed in Section IV-C, are mainly related to noisy force/torque measurements and to interaction events that involve more than a single contact point. In the experiments reported in the paper, the interaction forces were produced manually using a tool with a small tip to make sure that the contact activated a small number of taxels. As a result the data collection was quite tedious and time consuming. We are at the moment planning to make the calibration completely autonomous. To enforce the hypothesis that contacts occur only at single points it is possible to proceed along two directions. First by checking that contacts indeed occur only in few (or at most one) taxels, and filter all the contact events that do not satisfy this hypothesis. Second, by maximizing the chances that this kind of events occurs. Along the lines of [10], we are planning to implement a motion control law that controls the robot so that it comes into contact with a small, fixed object. In this scenario both the proposed calibration methods are applicable. The advantage of an autonomous procedure is that it will allow to collect a larger amount of data, which will help to improve the quality of the final results.

We are also investigating the possibility to add other constraints to the problem formulation in order to improve the precision of the final results. Instead of specifying the exact surface on which the skin is mounted, we could simply constrain that surface to be smooth. Moreover, since we know that the distance between neighbouring taxels is within certain limits (approximately 4 mm to 6 mm), we could use this information as a constraint.

Finally, the 84 taxels located on the upper part of the iCub forearm sufficed to test the presented approaches. Nonetheless, the iCub is equipped with a much larger amount of tactile elements, and even more are going to be mounted on it, covering the arms, torso and legs. In the future, the proposed calibration procedure will be tested on this massive tactile sensor network, resulting in a complete 3D map of the whole body of the robot.

VI. Acknowledgments

The authors would like to thank Arjan Gijsberts and Alessandro Scalzo for their support and Matteo Fumagalli and Marco Randazzo for their work on the force/torque sensor.

References

[1] G. Metta, G. Sandini, D. Vernon, L. Natale, and F. Nori, "The iCub humanoid robot: an open platform for research in embodied cognition," in *Workshop on Performance Metrics for Intelligent Systems, National Institute of Standards and Technology*. Washington DC, USA: ACM, 2008.

[2] H. Marques, M. Jantsch, S. Wittmeier, O. Holland, C. Alessandro, A. Diamond, M. Lungarella, and R. Knight, "ECCE1: the first of a series of anthropomimetic musculoskeletal upper torsos," in *Humanoid Robots (Humanoids), 2010 10th IEEE-RAS International Conference on*, Nashville, TN, USA, 2010, pp. 391 – 396.

[3] G. Hoffman and G. Weinberg, "Gesture-based human-robot jazz improvisation," in *Robotics and Automation (ICRA), 2010 IEEE International Conference on*. IEEE, 2010, pp. 582–587.

[4] V. Lumelsky, *Sensing, intelligence, motion: how robots and humans move in an unstructured world*. Wiley-Blackwell, 2006.

[5] T. Taichi, M. Takahiro, I. Hiroshi, and H. Norihiro, "Automatic Categorization of Haptic Interactions-What are the Typical Haptic Interactions Between a Human and a Robot?" in *Humanoid Robots, 2006 6th IEEE-RAS International Conference on*. IEEE, 2006, pp. 490–496.

[6] Y. Ohmura, Y. Kuniyoshi, and A. Nagakubo, "Conformable and scalable tactile sensor skin for curved surfaces," *Proceedings 2006 IEEE International Conference on Robotics and Automation, 2006. ICRA 2006.*, no. May, pp. 1348–1353, 2006.

[7] G. Cannata, M. Maggiali, G. Metta, and G. Sandini, "An embedded artificial skin for humanoid robots," *2008 IEEE International Conference on Multisensor Fusion and Integration for Intelligent Systems*, pp. 434–438, Aug. 2008.

[8] E. Baglini, G. Cannata, and F. Mastrogiovanni, "Design of an embedded networking infrastructure for whole-body tactile sensing in humanoid robots," in *Proc. of 2010 IEEE-RAS Int.l Conf. on Humanoid Robots (Humanoids2010)*, Nashville, TN, USA, 2010, pp. 671–676.

[9] A. Schmitz, P. Maiolino, M. Maggiali, L. Natale, G. Cannata, and G. Metta, "Methods and Technologies for the Implementation of Large Scale Robot Tactile Sensors," *accepted for publication on Robotic Sense of Touch special issue in IEEE Transactions on Robotics*, 2011.

[10] G. Cannata, S. Denei, and F. Mastrogiovanni, "Towards automated self-calibration of robot skin," in *Robotics and Automation (ICRA), 2010 IEEE International Conference on*. IEEE, 2010, pp. 4849–4854.

[11] D. Pierce, "Map learning with uninterpreted sensors and effectors," *Artificial Intelligence*, no. 003658, pp. 1–47, 1997.

[12] Y. Kuniyoshi, Y. Yorozu, Y. Ohmura, K. Terada, T. Otani, A. Nagakubo, and T. Yamamoto, "From humanoid embodiment to theory of mind," *Embodied artificial intelligence*, pp. 629–629, 2004.

[13] T. Noda, T. Miyashita, H. Ishiguro, and N. Hagita, "Super-Flexible Skin Sensors Embedded on the Whole Body, Self-Organizing Based on Haptic Interactions," *Proc. of Robotics: Science and Systems IV*, 2008.

[14] J. Modayil, "Discovering sensor space: Constructing spatial embeddings that explain sensor correlations," in *Development and Learning (ICDL), 2010 IEEE 9th International Conference on*. IEEE, 2010, pp. 120–125.

[15] A. Bicchi, J. K. Salisbury, and D. L. Brock, "Contact Sensing from Force Measurements," *The International Journal of Robotics Research*, vol. 12, no. 3, pp. 249–262, June 1993.

[16] B. Eberman and J. K. Salisbury, "Determination of manipulator contact information from joint torque measurements," in *Experimental Robotics I*. Springer, 1990, pp. 463–473.

[17] A. Bjorck, *Numerical methods for least squares problems*. Society for Industrial Mathematics, 1996.

[18] M. Fumagalli, M. Randazzo, F. Nori, L. Natale, G. Metta, and G. Sandini, "Exploiting proximal F/T measurements for the iCub active compliance," in *Intelligent Robots and Systems (IROS), 2010 IEEE/RSJ International Conference on*. IEEE, 2010, pp. 1870–1876.